



The small Cherenkov array added by new observation points is located in a center of the main array. The observation points are located symmetrically relative to the center of the main array and form a net of the equilateral triangles the sides of 50, 100, 250, 500 m. The EAS events are selected by the coincidence of responses from three Cherenkov detectors located at the tops of equilateral triangles for the time of 2,5 ms. For showers with  $E_0 > 10^{17}$  eV the small array operates synchronously with the large array. Since the operation of the small Cherenkov array we carried out observations of the EAS Cherenkov during  $\sim 2716$  hour observations and registered  $\sim 2,5 \cdot 10^5$  eV EAS events with energies above  $10^{15}$  eV. The showers are selected by the parameter  $Q(100)$  - the density of the Cherenkov light flux at a distance of 100 m of the shower core. This parameter, as the calculations (Belayev et al., 1980) have shown, depends weakly on a zenith angle and is measured in every shower. The transition to the shower primary energy has been made according to the formula:

$$E_0 = (5,2 \pm 1,1) \cdot (Q(100)/10^7)^{0,96 \pm 0,02} \quad (1)$$

which is obtained by the calorimetric method (Afanasiev et al., 1993). In Eq. (1) the condition of the atmosphere are taken into account.

### 3 Results and Discussion

By the measurement results the EAS spectra have been constructed by the  $Q(100)$  and  $N_s(0^\circ)$  parameters. Here  $N_s(0^\circ)$  is the total particle number at sea level. The transition to the vertical has been carried out by the barometric height formula:

$$N_s(0^\circ) = N_s(\theta) \cdot \exp(X_0(\sec\theta - 1)/\lambda), \quad (2)$$

where  $\lambda$  is the charged particles absorption path being equal to

$$\lambda = (215 \pm 20) + (10 \pm 3) \cdot \lg(N/10^6) + 150 \cdot (\sec\theta - 1) \quad (3)$$

The dependence (3) has been obtained from the correlation analysis of the  $N_s$  and  $Q(100)$  parameters in showers arriving at various zenith angles (see in Part. 3). The transition from  $N_s$  to  $E_0$  has been carried out by the formula

$$N_s(0^\circ) = (5,74 \pm 1,15) + (1,10 \pm 0,02) \cdot \lg(Q(r = 100)/10^6) \quad (4)$$

and by using (1). The differential EAS spectrum by the  $N_s$  parameter has the irregularity at  $N_s \sim (3,3 \pm ,8) \cdot 10^5$  of particles in a simple power presentation has the following power indices: before the knee ( $\gamma_1 = -2,42 \pm 0,03$ ) and after the knee ( $\gamma_2 = -2,85 \pm 0,02$ ). Fig.2 presents the differential cosmic ray energy spectrum. It is seen that the region of the spectrum irregularities falls on the energy interval  $(2 \div 4) \cdot 10^{15}$  eV (i.e. at  $Q(100) \sim (6,5 \pm 1,0) \cdot 10^5$  phot. / m<sup>2</sup>). If we approximate the spectrum by a simple power law then the power index before

the knee is  $\beta_1 = (-2,63 \pm 0,03)$ , and after the knee is  $\beta_2 = (-3,12 \pm 0,02)$ .

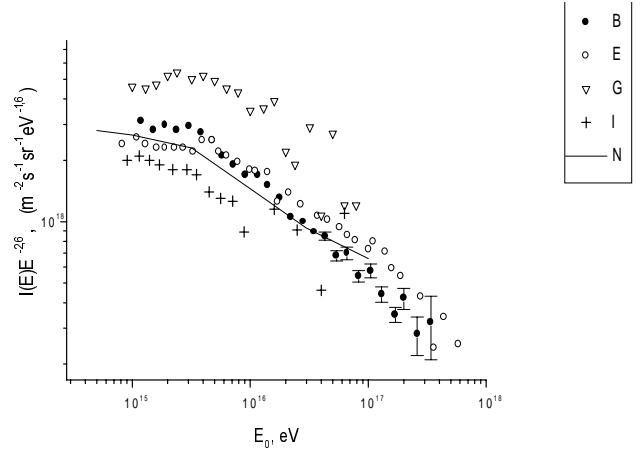


**Fig.2.** The differential energy cosmic ray spectrum. B is our result;

E – is the Akeno array (Nagano et al., 1984); G – is the Tunka array (Gress et al., 1999); I – is the CASA – BLANCA array (Fowler et al., 2000); N – is the KASCAD array (Kampert et al., 2000).

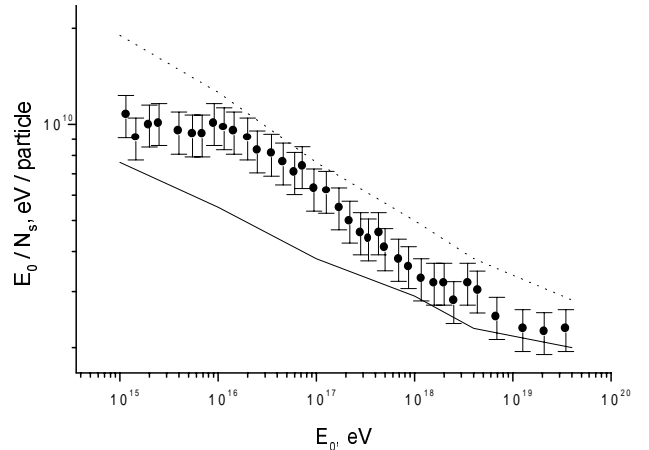


**Fig.3.** Dependence of the ratio  $E_0/N_s$  on primary energy  $E_0$ . Curves:

primary protons (---) and primary nuclei of iron (...). Calculations by the QGSJET model (Knurenko et al, 1999).

The differential energy spectrum obtained using (2), (3), (4) from the spectrum by the  $N_s$  parameter within the experimental errors coincides with the spectrum obtained from the EAS spectrum by the  $Q(100)$  parameter. If we consider the spectrum form in detail then it is necessary to mark a step the intensity doesn't change practically in the energy range of  $10^{16} \div 2 \cdot 10^{16}$  eV. Such a form of the spectrum is also observed by data from other arrays (see Fig. 2). But it is prematurely to say unambiguously about a thin spectrum structure in the interval  $10^{16} \div 2 \cdot 10^{16}$  eV. Firstly, the spectra measured at various arrays coincide well by a form, but considerably differ in intensity. Secondly, some compact EAS arrays have different registration effectiveness of showers at  $E_0 < 10^{16}$  and  $E_0 > 10^{16}$  eV. It may occur that this effect is connected with a different measurement methods, calculations of intensity and shower energy. By our opinion, the most correct method is the determination of the shower primary energy by the EAS Cherenkov radiation flux because the model of the EAS development is not yet known.

Fig.3 shows the coefficient  $k$  from formula  $E_0 = k \cdot N_s$  versus the primary energy. The result is obtained by the averaging of a great number of showers registered at small and large arrays. Only 20 % systematic errors in determination of  $E_0$  are shown. In Fig.3 the calculations by the QGSJET model for the primary protons and iron nuclei are given. The calculations are carried out for the fixed energies  $10^{15}$ ,  $10^{16}$ ,  $10^{17}$ ,  $3 \cdot 10^{17}$ ,  $10^{18}$ ,  $5 \cdot 10^{18}$ ,  $10^{19}$  and  $3 \cdot 10^{19}$  eV (Knurenko et al., 1999). The thresholds of the scintillation ( $0,5 \text{ particl/m}^2$ ), Cherenkov ( $15$  and  $8 \text{ phot./cm}^2$ ) detectors and selection peculiarities of the EAS event by the array have been taken into account. For every energy about 500 EAS events at zenith angles  $\theta = 10, 20, 30, 40, 50$  and  $60^\circ$  have been simulated. Then, to find the EAS parameters the a

standard program of the treatment and analysis of showers is used. From Fig.3 one can make a conclusion that the knee in the cosmic ray energy spectrum at  $E_0 \sim 3 \cdot 10^{15}$  eV is probably connected with the change of the mass composition of primary particles if the QGSJET model is true for the description of the EAS development of such energies. Perhaps, the next analysis of all EAS components at a fixed energy including fluctuations the distribution form of the shower parameters and their correlation's will help to resolve this task.

## References

- Afanasiev B.N. et al. // Proc. ISEHECR: Astrophysics and Future Observatories. Tokyo (1996), p. 412.  
 Afanasiev B.N. et al. // Proc. Tokyo Workshop on Techniques for the Study of Extremely High Energy Cosmic Rays. Tokyo (1993), p. 35.  
 Belayev, A.A., Ivanenko, I.P., Kanevsky, B.L. et al., M.: Nauka., Electron - Photon cascade of Cosmic Rays for Highest Energy., 305p (1980).  
 Berezhko E.G., Krymsky G.F. // VFH, 1988, v. 154, p. 49.  
 Efimov N.N. Thesis. MSU NIYAF (1967).  
 Erlykin A.D., Wolfendale A.W. // Astroparticle Physics, 7, 1 (1997).  
 Fowler J.W. et al. // arXiv:astro-ph/0003190 v2.  
 Gress O.A. et al. // Nucl. Phys. B (Proc. Suppl.) 75A (1999), p. 299.  
 Kampert K.-H. et al. // arXiv:astro-ph/0102266.  
 Knurenko S.P., Sleptsova V.R., Kalmykov N.N. et al. // Proc. 26<sup>th</sup> ICRC, v.1 (1999), p. 372.  
 Nagano M. et al. // J. Phys. G., 10, 1295 (1984).  
 Nikolsky S.I. Preprint FIAN. 15 (1992).  
 Pogorely V.G. Thesis. MSU (1992).